

New GOES Imager System Products Suitable for Use on Field-Deployable Systems

Stanley Q. Kidder, Kenneth E. Eis*, and Thomas H. Vonder Haar

Cooperative Institute for Research in the Atmosphere

Colorado State University, Fort Collins CO 80523-1375

kidder@cira.colostate.edu

Objective and Relevance: Recent research has yielded three satellite-based values of significance to the military. These three are isotropic albedo, 3.9 μm albedo, and surface skin temperature. Isotropic albedo is used to correct for cloud reflection near the terminator. This correction factor allows the forecaster to get a better display of clouds at dawn and dusk when many strike operations occur. The 3.9 μm albedo provides a clear discriminator for fog, stratus, and CI clouds. The surface skin temperature gives the EOTDA weapons planner the IR temperature for the background, so critical to target contrast analysis and in the calculation of the background to target inversion time. Past EOTDA support has relied on knowledge of surface features, moisture, and soil structure to estimate skin temperature. Now it can be directly measured.

Research Accomplished: The algorithms calculate (1) isotropic albedo, (2) 3.9 μm albedo, (3) surface skin temperature, and (4) a blended product consisting of 3.9 μm albedo at night and isotropic albedo during the day. They are presented in the next four sections.

Isotropic albedo. The isotropic albedo product is the familiar GOES visible image corrected for solar zenith angle. It is especially useful near sunrise and sunset for analyzing cloud fields. The isotropic albedo can be extracted as follows.

The raw, 10-bit, GOES Variable (GVAR) count (0-1023) measured by the GOES Imager can be converted to a reflectance, R , by the calibration equations of Weinreb et al. (1998). This reflectance would be the albedo *if the sun were overhead at every point*. It is not, of course, but it is easy to correct for the variation in solar angle. We do two things to the reflectance: (1) multiply by the secant of the solar zenith angle and (2) multiply by the square of the ratio of the earth-sun distance to the mean earth-sun distance. The latter correction is small (within $\pm 3.4\%$) but easily accomplished because it is a byproduct of the zenith angle calculation. In equation form,

$$\text{Isotropic albedo} = R(d/d_{\text{mean}})^2 \sec \zeta \quad (1)$$

where ζ is the solar zenith angle, d is the earth-sun distance, and d_{mean} is the annual-average earth-sun distance. We call the result the *isotropic albedo* because it does not take into account bidirectional effects, i.e., it is what the albedo would be if the scene were an isotropic reflector, one which reflects uniformly in all directions. This is not a new calculation. It has been done for many years by people who study the radiation budget of earth and others (see chapter 10 of Kidder and Vonder Haar 1995 for an explanation and bibliography).

Figure 1 compares the normal visible image display (uncorrected albedo) with the isotropic albedo. The clouds are similar in the southeastern part of the images, but near the terminator, the clouds disappear into the dark background in the top image. The cloud information in the dark area is not totally lost; it can be brought out of the normal image with image enhancement techniques (e.g. “stretching”), but only by over brightening the rest of the image. The isotropic albedo can be viewed as a physically based enhancement, which brings out the clouds (the meteorologically important features in the image) uniformly across the image. A good example of this is seen in the cirrus clouds over Kansas, Oklahoma, and Texas. Note that the bright band

near the terminator is a bidirectional effect, the result of the fact that at low sun elevation angles (high zenith angles) clouds are not isotropic reflectors.

The chief use of the isotropic albedo product is in analyzing clouds, especially near sunrise and sunset. This product could also be useful in constructing cloud climatologies (Reinke et al. 1992; Gould and Fuelberg 1996) because the threshold for distinguishing clouds is much less strongly related to sun angle than in the uncorrected visible image.

3.9 μm albedo. The so-called “fog product” has revolutionized fog and liquid water cloud detection at night. As described by Ellrod (1995), liquid water clouds have a lower emittance (emissivity) at 3.9 μm (GOES channel 2) than at 10.7 μm (channel 4). Whereas the emittance of a “thick” liquid water cloud at 10.7 μm is near 1.0, the emittance at 3.9 μm is near 0.7. The result is that at night, the brightness temperature at 3.9 μm ($T_{3.9}$) is less than that at 10.7 μm ($T_{10.7}$). This difference ($T_{10.7} - T_{3.9}$) has been exploited to produce the “fog product.”

Emittance and albedo are related: they sum to one. Therefore, liquid water clouds with a 3.9 μm emittance of about 0.7 have an albedo of about 0.3. Solar radiation at 3.9 μm is not negligible, as it is at 10.7 μm . When the sun comes up, liquid water clouds reflect solar radiation to the satellite, and it appears that the clouds warm. $T_{3.9}$ becomes larger than $T_{10.7}$. In the fog product, liquid water clouds turn black due to the reflected solar radiation. To handle this problem, the “reflectance product” has been developed (Dills et al. 1996).

Because the reflection of solar radiation in the daytime and the lowered brightness temperatures at night over liquid water clouds are caused by the same phenomenon (decreased emittance / increased albedo), it is possible to develop a simple, unified product which is applicable both day and night. The radiance measured by the GOES Imager at 3.9 μm is composed of reflected and emitted parts. The emitted part can be approximated as

$$\text{Emitted radiation} = \varepsilon_{3.9} B_{3.9}(T_{10.7}) = (1 - A_{3.9}) B_{3.9}(T_{10.7}), \quad (2)$$

where $A_{3.9}$ is the 3.9 μm albedo. The reflected radiation starts with the 3.9 μm solar irradiance of the scene, which can be approximated as

$$\text{Solar irradiance} = B_{3.9}(T_{\text{sun}}) \Omega_{\text{sun}} \cos\zeta, \quad (3)$$

where Ω_{sun} is the solid angle of the sun subtended at the earth (6.8×10^{-5} sr), and, based on Thekaekara (1972), $T_{\text{sun}} = 5888$ K at 3.9 μm . The radiance reflected to the satellite from a particular point or location is the product of the bidirectional reflectance and the solar irradiance. Assuming that the point is an isotropic surface, the bidirectional reflectance is simply $\pi^{-1}A_{3.9}$ (see Kidder and Vonder Haar 1995, pp.79-81, for details). Thus, the reflected radiation is simply:

$$\text{Reflected radiation} = \pi^{-1} A_{3.9} B_{3.9}(T_{\text{sun}}) \Omega_{\text{sun}} \cos\zeta. \quad (4)$$

Therefore, the radiance measured by the satellite can be written as the sum of the emitted and reflected radiation:

$$L_{3.9} = \pi^{-1} A_{3.9} B_{3.9}(T_{\text{sun}}) \Omega_{\text{sun}} \cos\zeta + (1 - A_{3.9}) B_{3.9}(T_{10.7}), \quad (5)$$

or, solving for $A_{3.9}$,

$$A_{3.9} = \frac{L_{3.9} - B_{3.9}(T_{10.7})}{\pi^{-1} B_{3.9}(T_{\text{sun}}) \Omega_{\text{sun}} \cos\zeta - B_{3.9}(T_{10.7})}. \quad (6)$$

At night ($\zeta > 90^\circ$) the same equation applies if we simply set $B_{3.9}(T_{\text{sun}}) = 0$.

To construct the 3.9 μm albedo product, GOES Imager data for channels 2 and 4 are processed using eq. (6). Then 3.9 μm albedos from -50% to $+50\%$ are displayed as a gray scale from black to white. Negative albedos result from thin cirrus, probably because of inhomogeneities in the partially transparent cirrus, which result in $T_{3.9}$ being larger than $T_{10.7}$.

Figure 2 shows the 3.9 μm albedo product for three times spanning sunrise. Land and ocean have near zero 3.9 μm albedo and thus appear gray. Liquid water clouds appear white, and cirrus appears black at night. With the exception of cirrus, there are no large changes between day and night. Eq. (6) has a problem just after sunrise, when the denominator goes from negative, through zero, to positive. This causes an anomaly in the displayed image.

Lee et al. (1997) have also discussed a day/night 3.9 μm product. The Lee et al. derivation is much more complicated than the 3.9 μm albedo presented in this paper.

The chief use of the 3.9 μm albedo product is in locating liquid water clouds/fog, especially at night.

Surface temperature. The third product to be described in this paper is called the surface temperature product (T_{sfc}). Based on the work of McMillin and Crosby (1984), the split widow channels (channel 4, 10.7 μm ; and channel 5, 12.0 μm , on the GOES Imager) can be used together to correct one of them for the effects of atmospheric absorption. The formula is

$$T_{\text{sfc}} = T_{10.7} + \eta(T_{10.7} - T_{12.0}), \quad (7)$$

where,

$$\eta = \frac{1 - \tau_{10.7}}{\tau_{10.7} - \tau_{12.0}}, \quad (8)$$

and τ is atmospheric transmittance (see Kidder and Vonder Haar 1995, pp. 219–225, for details). MODTRAN (Berk et al. 1989) calculations for the standard mid-latitude atmosphere show that for the GOES Imager $\tau_{10.7}$ is about 0.68 and $\tau_{12.0}$ is about 0.53, which means that η is approximately 2. This derivation is similar to sea surface temperature algorithms (McClain et al. 1985), but it is simpler. Figure 3 shows an example T_{sfc} image with the corresponding isotropic albedo image for comparison. T_{sfc} is mostly of value in humid situations to “clear” the water vapor from the satellite signal to reveal the surface (skin) temperature. T_{sfc} appears quite similar to the usual $T_{10.7}$ image, but with slightly more noise because it is a combination of two channels and therefore has compounded noise.

The chief use of the surface temperature product is to determine changes or boundaries in the low-level temperature. Color enhancement tables can be used to quickly quantify the surface temperatures and help track changes.

Day/night albedo. It is easy to combine the 3.9 μm albedo and the isotropic albedo to produce a day/night albedo product. The combined product displays the 3.9 μm albedo when the sun is down and the isotropic albedo when the sun is up. Figure 4 shows that this product is particularly useful for monitoring low (liquid water) clouds across the terminator.

Although we have presented these four products as GOES products, nearly the same spectral channels are present on the Advanced Very High Resolution Radiometer (AVHRR) instrument on the polar-orbiting NOAA satellites. To convert AVHRR counts to radiances, see the *NOAA Polar Orbiter Data User's Guide* (1997) for the TIROS N and NOAA 6 through 14 satellites, or see the *NOAA KLM User's Guide* (1997) for NOAA 15 and higher. Because the channels are different, slightly different parameters are necessary: at 3.7 μm , $T_{\text{sun}} \approx 5827$ K (Thekaekara 1972), and $\eta \approx 3$ (Price 1984).

Conclusions and Recommendations: We have presented four simple products which can be constructed from GOES Imager data (or AVHRR data) to improve weather analysis and forecasting. They are the isotropic albedo product, the 3.9 μm albedo product, the surface temperature product, and the day/night albedo product. Each of these products has been tested using *GOES-8*, *GOES-9*, and *GOES-10* imagery. We believe that these are the type of products which should be available to forecasters. They are simple, easily produced, reliable, and physically based. These products extend the usefulness of the raw channel data from the GOES satellites. They are suitable for use on field-deployable systems, and they could be reconfigured from remote sites.

REFERENCES

- Berk, A., L. S. Bernstein, and D. C. Robertson, 1989: *MODTRAN: A Moderate Resolution Model for LOWTRAN 7*, U.S. Air Force Geophysics Laboratory Tech. Rep. GL-TR-89-0122, Hanscom AFB, Mass.
- Dills, P. N., D. W. Hillger, and J. F. W. Purdom, 1996: Distinguishing between different meteorological phenomena and land surface properties using the multispectral imaging capabilities of GOES-8. *Eighth Conf. on Satellite Meteorology and Oceanography*, American Meteorological Society, 339–342.
- Ellrod, G. P., 1995: Advances in the detection and analysis of fog at night using GOES multispectral infrared imagery. *Wea. Forecasting*, **10**, 606–619.
- Gould, K. J., and H. E. Fuelberg, 1996: The use of GOES-8 imagery and RAMSDIS to develop a sea breeze climatology over the Florida panhandle. *8th Conf. On Satellite Meteorology and Oceanography*, American Meteorological Society, Boston, 100–104.
- Kidder, S. Q., and T. H. Vonder Haar, 1995: *Satellite Meteorology: An Introduction*. Academic Press, San Diego, 466 pp.
- Lee, T. F., F. J. Turk, and K. Richardson, 1997: Stratus and fog products using GOES-8–9 3.9- μm data. *Wea. Forecasting*, **12**, 664–677.
- McClain, E. P., W. G. Pichel, and C. C. Walton, 1985: Comparative performance of AVHRR-based multichannel sea surface temperatures. *J. Geophys. Res.*, **90**, 11587–11601.
- McMillin, L. M., and D. S. Crosby, 1984: Theory and validation of the multiple window sea surface temperature. *J. Geophys. Res.*, **89**, 3655–3661.
- NOAA KLM User's Guide*, 1997: NOAA/NESDIS, Washington, DC. [Available on line at <http://perigee.ncdc.noaa.gov/docs/klm/index.htm>.]
- NOAA Polar Orbiter Data User's Guide*, 1997: NOAA/NESDIS, Washington, DC. [Available on line at <http://perigee.ncdc.noaa.gov/docs/podug/index.htm>.]
- Price, J. C., 1984: Land surface temperature measurements from the split window channels of the NOAA-7 Advanced Very High Resolution Radiometer. *J. Geophys. Res.*, **89**, 7231–7237.
- Reinke, D. L., C. L. Combs, S. Q. Kidder, and T. H. Vonder Haar, 1992: Satellite cloud composite climatologies: A new high-resolution tool in atmospheric research and forecasting. *Bull. Amer. Meteor. Soc.*, **73**, 278–285
- Thekaekara, M. P., 1972: *Photonics Spectra*, **6**, 32–35. [Data available from ftp://ftp.ngdc.noaa.gov/STP/SOLAR_DATA/ATM_HANDBOOK/]
- Weinreb, M. M. Jamieson, N. Fulton, Y. Chen, J. X. Johnson, J. Bremer, C. Smith, and J. Baucum, 1998: Operational calibration of Geostationary Operational Environmental Satellite-8 and -9 Imagers and Sounders. *Applied Optics*, **36**, 6895–6904.

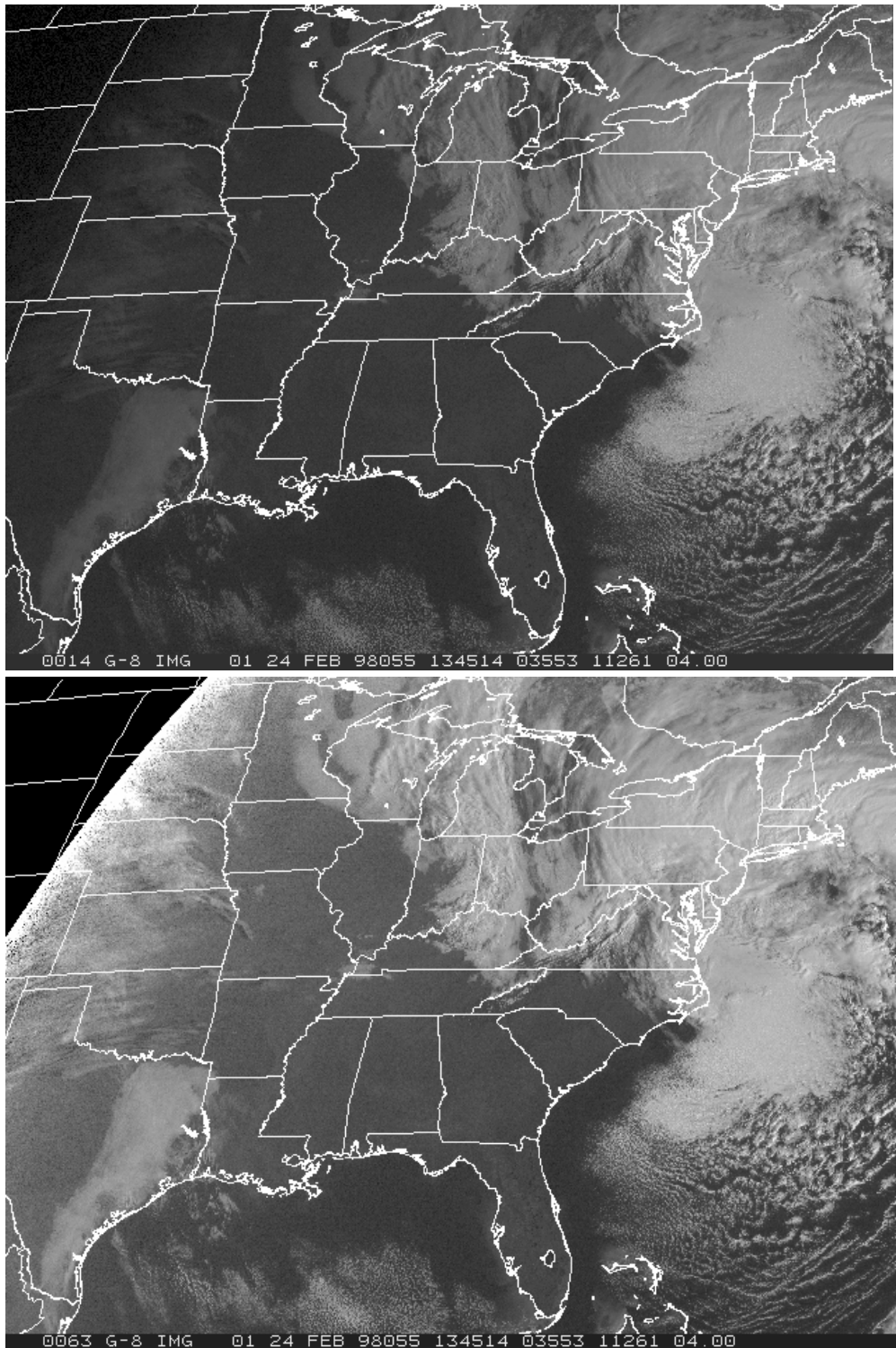


Figure 1. (Top) GOES visible image (channel 1, 0.67 μm). (Bottom) Isotropic albedo.

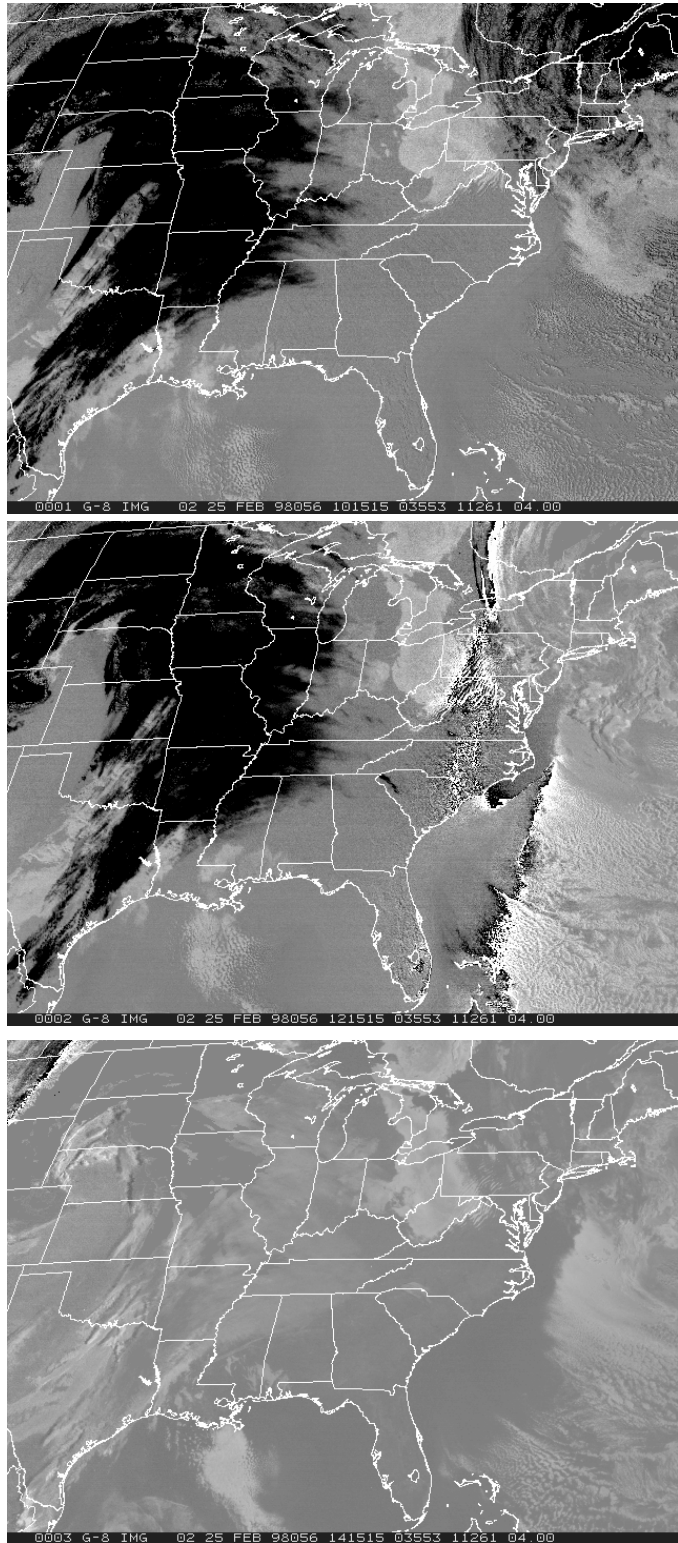


Figure 2. 3.9 μm albedo product for three times spanning sunrise: (top) 1015 UTC, (middle) 1215 UTC, (bottom) 1415 UTC.

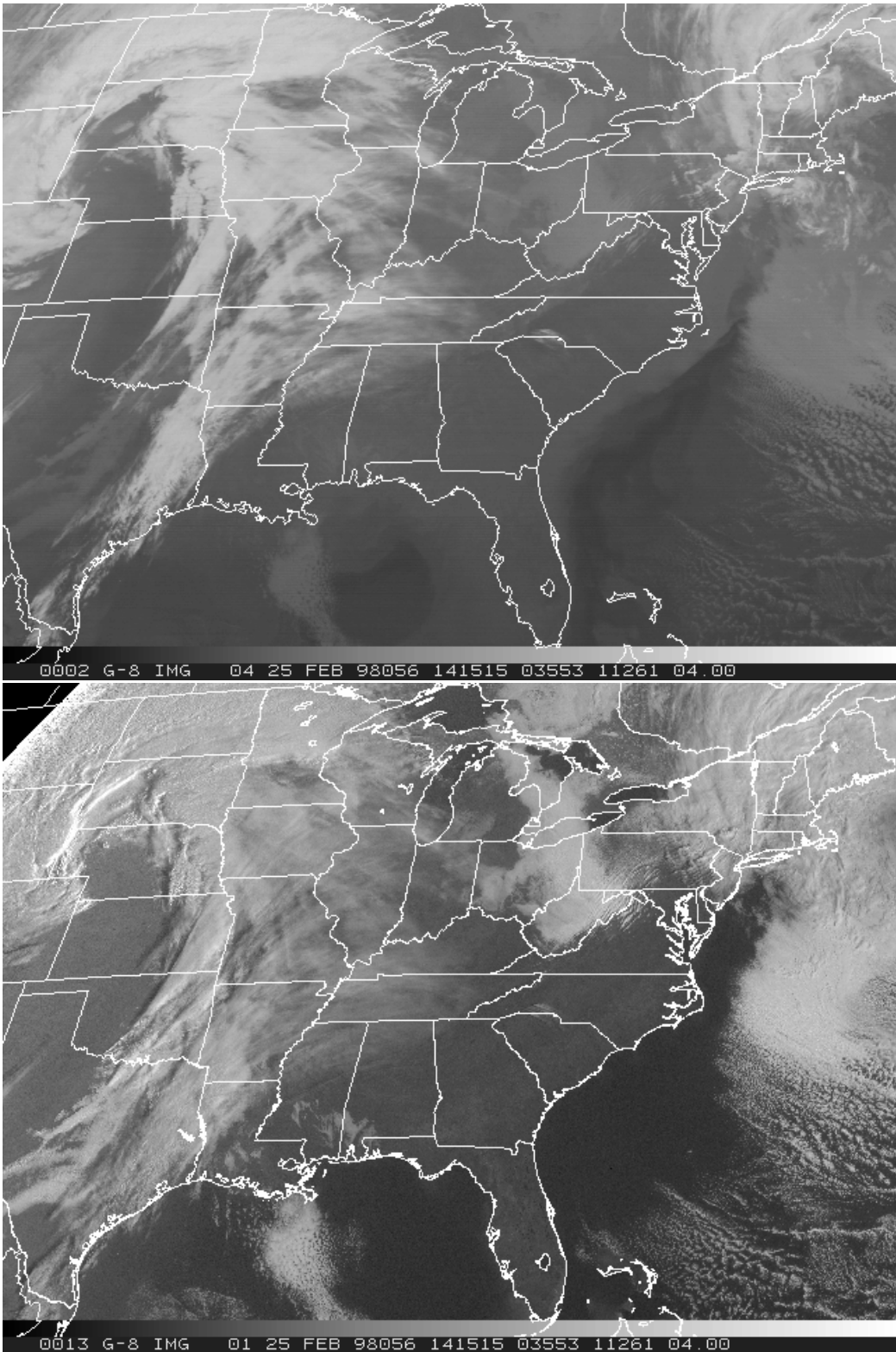


Figure 3. (Top) The surface temperature product. (Bottom) isotropic albedo.

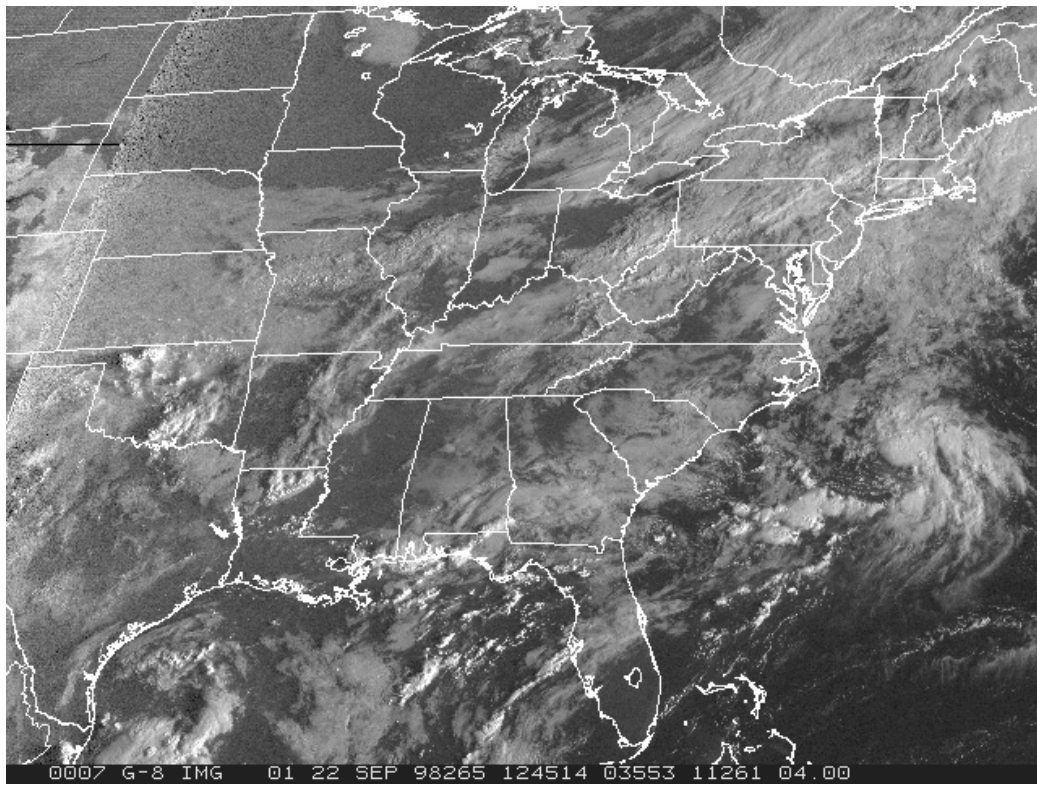
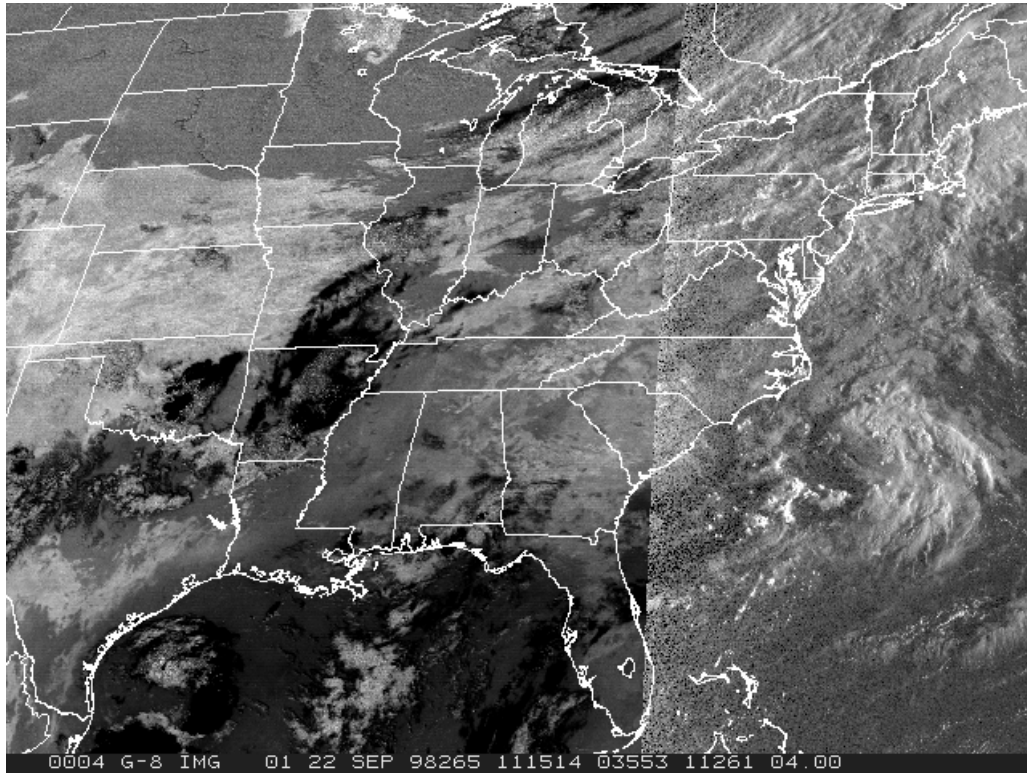


Figure 4. Day/night albedo product at two times: (top) 1115 UTC, (bottom) 1245 UTC.